Adv. Biophys., Vol. 34, pp. 25–39 (1997)

LATERAL FORCES ACTING BETWEEN PARTICLES IN LIQUID FILMS OR LIPID MEMBRANES

PETER A. KRALCHEVSKY

Laboratory of Thermodynamics and Physico-chemical Hydrodynamics, Faculty of Chemistry, University of Sofia, Sofia 1126, Bulgaria

It was recently established that attractive lateral capillary forces can be a crucial factor for the formation of two-dimensional (2D) ordered arrays of colloidal particles or protein macromolecules in liquid films (*1–4*). Forces of similar origin appear between inclusions (membrane proteins) incorporated in lipid bilayers (*5*). The latter forces can be expected to play a role in phenomena accompanied by aggregation of membrane proteins (endocytosis, immunoresponse and the processes of patching and capping, enzymatic reactions, intracellular interaction, *etc.*).

In the present article we first demonstrate the role of the lateral capillary forces in the process of 2D array formation. Then, we review the theory of these forces for the cases of liquid films and lipid membranes.

I. ON THE MECHANISM OF 2D ARRAY FORMATION

Interest in ordered 2D colloid structures is stimulated by their possible applications in optical devices (*6–9*) and some other techniques like data storage, microelectronics, and synthetic membrane production. Moreover, the 2D crystallisation provides a possibility for investigating the structure of globular and, especially, membrane proteins (*10–14*).

2D arrays from micrometer (*1, 7, 8*) and sub-micrometer (*7, 9, 15*) latex particles, from proteins and protein complexes (*16–26*), and even from viruses (*10, 21*), were obtained and their structure was analysed.

To reveal the mechanism of formation of 2D arrays we carried out the following experiment (*1*). A layer of thickness h formed from an aqueous suspension of latex particles (diameter 1.7 μm) is observed by microscope through the glass substrate. When h is greater than the particle diameter one observes the Brownian motion of the particles. The layer thickness h is allowed to decrease due to water evaporation. Suddenly, at the moment when h becomes equal to the particle diameter one observes a transition from disorder to order (Fig. 1). This transition is triggered by the lateral capillary forces which are due to the overlap of the menisci formed around the particles (*2–4*). Indeed, the 2D crystallisation always started when the thickness of the water layer became equal to the particle diameter. This implies that the 2D-crystal nuclei are formed under the capillary attraction arising when the tops of the particles protrude from the water layer (Fig. 2). The attraction energy can be much larger than the thermal energy (kT) even with nanometre-sized particles (*4*).

We were able to show (*1*) that the crystal growth is caused by a convective transport of particles towards the ordered nucleus. This effect appears when menisci (Fig. 2) form around the protruding tops of the hydrophilic particles in the nucleus. These menisci hinder the

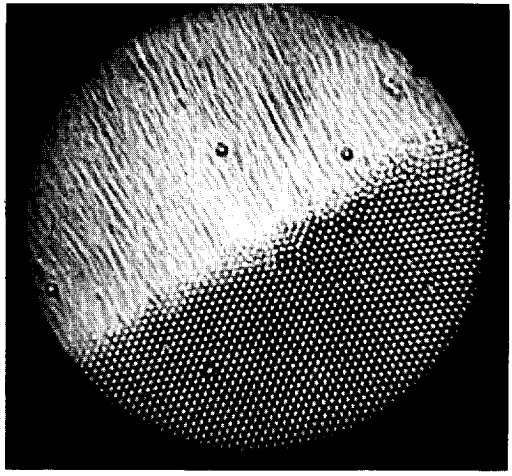

Fig. 1. Photograph of the growth of 2D array from latex particles (diameter 1.7 μm): the tracks of the particles rushing towards the ordered phase are seen.

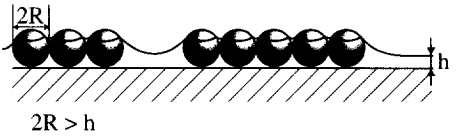

Fig. 2. 2D ordering of suspension particles in a liquid film: capillary forces appear and cause aggregation after the particle tops protrude from the film.

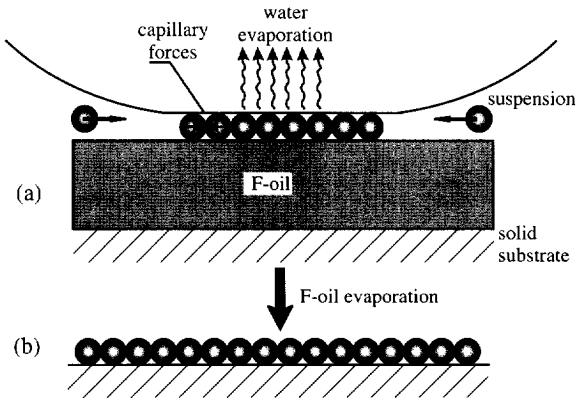

Fig. 3. Experimental set up for 2D array formation on F-oil substrate: (a) 2D ordering of particles in an aqueous film over F-oil; (b) the formed 2D array is deposited on a solid substrate after the evaporation of the water and the F-oil.

further thinning of the water layer in the nucleus. An intensive water influx from the thicker parts of the layer, which tends to compensate the water evaporation from the nucleus, appears next. This flux carries the suspended particles towards the nucleus. By decreasing or increasing the water evaporation rate we could speed up or slow down the convective particle transport. At increased humidity, we saw a complete arrest of the process of ordering and even disintegration of the already ordered clusters.

We investigated also the possibility for application of perfluorinated oil (F-oil) as a liquid substrate for 2D array formation (*27*). We use perfluormethyldecalin (PFMD) which possesses some of the appropriate features of the mercury substrate used in refs. *22* and *23* (molecularly smooth and tangentially mobile surface) and some additional advantages: (i) it is chemically inert and hazardless (*28–30*); (ii) it allows the merging and rearranging of already ordered domains into larger ones, (iii) the 2D structure formed can be gently deposited onto another surface after evaporation of all F-oil, and (iv) it is difficult to

contaminate the fluorocarbon surface insofar as the common surfactants adsorb poorly at the fluorocarbon-water interface (*31*). As a final result, large and well ordered domains from latex particles and clusters from ferritin molecules are obtained under appropriate conditions and after that are transferred onto a solid substrate (Fig. 3), which can be the specimen grid of the electron microscope.

II. CAPILLARY FORCES IN LIQUID FILMS

The origin of the lateral capillary forces is the deformation of the liquid surface, which is supposed to be flat in the absence of particles. The larger the interfacial deformation created by the particles, the stronger the capillary interaction between them. In the pioneering work of Nicolson (*32*) the capillary interaction energy between two bubbles attached to a liquid surface was calculated by assuming that the surface deformation is a mere superposition of the deformations created by the single bubbles (superposition approximation). Later several theoretical studies were published concerning the interaction between spheres floating on a single interface (*33*) (where the superposition approximation was used) or between two infinite horizontal cylinders laying on an interface (*33, 34*).

In our work we extended the theory further by solving analytically the linearized Laplace equation (at small slopes of the meniscus around the particles) in bicylindrical coordinates (*2–4, 35*). General expressions were obtained for the capillary interaction energy and force between two vertical cylinders and between two spheres (*2, 3, 35*),

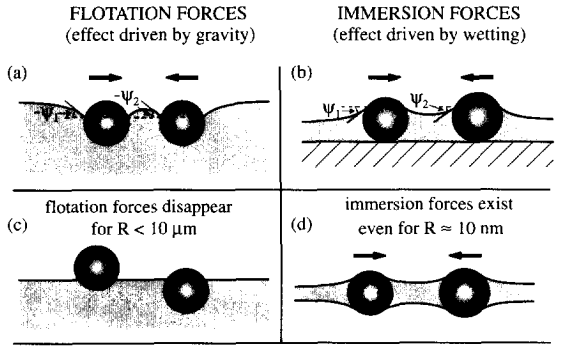

Fig. 4. Flotation (a, c) and immersion (b, d) lateral capillary forces due to the overlap of the menisci formed around particles captured in liquid films.

between a sphere and a vertical wall (*36, 37*), and other configurations (*3, 35*).

It is known that two similar particles floating on a liquid interface attract each other (*33, 35*) (see Fig. 4a). This attraction appears because the liquid meniscus deforms in such a way that the gravitational potential energy of the two particles decreases when they approach each other. Hence the origin of this force is the *particle weight* (including the Archimedes force).

On the other hand, we established that force of capillary attraction appears also when the particles (instead of freely floating) are partially immersed in a liquid layer on a substrate (*2–4*) (see Fig. 4b). The deformation of the liquid surface in this case is related to the *wetting properties* of the particle surface, *i.e.* to the position of the contact line and the magnitude of the contact angle, rather than to gravity.

To distinguish between the capillary forces in the case of floating particles and in the case of partially immersed particles on a substrate, we called the former lateral *flotation* forces and the latter lateral *immersion* forces (*4, 35*). These two kinds of force exhibit similar dependence on the interparticle separation but very different dependencies on the particle radius and the surface tension of the liquid. The flotation and immersion forces can be both attractive and repulsive. This is determined by the signs of the meniscus slope angles ψ_1 and ψ_2 at the two contact lines: the capillary force is attractive when $\sin\psi_1 \sin\psi_2 > 0$ and repulsive when $\sin\psi_1 \sin\psi_2 < 0$. In the case of flotation forces, $\psi > 0$ for *light* particles (including bubbles) and $\psi < 0$ for *heavy* particles. In the case of immersion forces between particles protruding from an aqueous layer, $\psi > 0$ for *hydrophilic particles* and $\psi < 0$ for *hydrophobic particles*. When $\psi = 0$ there is no meniscus deformation and, hence, there is no capillary interaction between the particles. This can happen with floating particles when the weight of the particles is too small to create significant surface deformation (Fig. 4c). The immersion force appears not only between particles in wetting films (Fig. 4b), but also in symmetric fluid films (Fig. 4d). The theory (*3, 4, 33*) provides the following asymptotic expression for calculating the lateral capillary force between two particles of radii R_1 and R_2 separated by a centre-to-centre distance L

$$F = 2\pi\sigma Q_1 Q_2 q K_1(qL)[1 + O(q^2 R_k^2)] \qquad r_k \ll L \tag{1}$$

where σ is the liquid-fluid interfacial tension, r_1 and r_2 are the radii of the two contact lines and $Q_k = r_k \sin\psi_k$ $(k = 1,2)$ is the "capillary charge" of the particle (*4, 35*); in addition,

$$\begin{aligned} q^2 &= \Delta\rho\, g/\sigma \qquad \text{(in thick film)} \\ q^2 &= (\Delta\rho\, g - \Pi')/\sigma \qquad \text{(in thin films).} \end{aligned} \tag{2}$$

Here, $\Delta\rho$ is the difference between the mass densities of the two fluids and Π' is the derivative of the disjoining pressure with respect to the film thickness; K_1 is the modified Bessel function. The asymptotic form of Eq. (1) for $qL \ll 1$ ($q^{-1} = 2.7$ mm for water),

$$F = 2\pi\sigma Q_1 Q_2 / L \qquad r_k \ll L \ll q^{-1} \tag{3}$$

looks like a two-dimensional analogue of Coulomb's law, which explains the name "capillary charge" of Q_1 or Q_2. Note that the immersion and flotation forces exhibit the same functional dependence on the interparticle distance, see Eqs. (1) and (3). On the other hand, their different physical origin results in different magnitudes of the "capillary charges" of these two kinds of capillary force. In this aspect they resemble the electrostatic and gravitational forces, which obey the same power law, but differ in the physical meaning and magnitude of the force constants (charges, masses). In the particular case when $R_1 = R_2 = R$; $r_k \ll L \ll q^{-1}$ one can derive (*4, 35*)

$$\begin{aligned} F &\propto (R^6/\sigma) K_1(qL) \quad \text{for flotation force} \\ F &\propto \sigma R^2 K_1(qL) \qquad \text{for immersion force.} \end{aligned} \tag{4}$$

Hence, the flotation force decreases, while the immersion force increases when the interfacial tension σ increases. Additionally, the flotation force decreases much more strongly with the decrease of R than the immersion force. Thus $F_{\text{flotation}}$ is negligible for $R < 10$ μm, whereas $F_{\text{immersion}}$ can be significant even when $R = 10$ nm. Hence, the immersion forces may be one of the main factors causing the observed self assembly of small colloidal particles (Fig. 1) and protein macromolecules (*22, 23*) confined in thin liquid films.

We extended the theory of the lateral capillary forces also to the case of particles captured in a *spherical* (rather than planar) thin liquid film or vesicle (*38*).

Lateral capillary forces between vertical cylinders or between spherical particles have been measured by means of sensitive electromechanical balance (*39*), piezo-transducer balance (*40*), and torsion micro-balance (*41, 42*). Good agreement between theory and experiment has been established (*40–42*).

III. CAPILLARY FORCES BETWEEN INCLUSIONS IN LIPID MEMBRANES

1. Biophysical Background

It was experimentally established that some integral proteins may aggregate in native membranes to form 2D crystals (*11–13, 43, 44*). Two well-known examples are the bacteriorhodopsin in the membranes of *Halobacterium halobium* (*11, 12*) and the connexons in the communicating cells (*13, 43*). Many proteins are also known to function in the non-aggregate state. Thus, properties of the rhodopsin from retinal rod membranes change significantly upon aggregation and immobilisation (*45*).

A particular type of non-specific interaction between integral proteins is mediated by their lipid environment, the so-called "lipid mediated interaction" (*46–48*). The main idea for such an interaction comes from the experimental observations that the proteins perturb the neighbouring lipid molecules (*49–53*). Theoretical models have been developed by Marcelja (*46*), Schröder (*47*), and Owicki *et al.* (*54, 55*).

Experiments performed by means of ESR and NMR methods specified the complex picture of the protein-lipid interaction. It was shown that the exchange rate of the lipids contacting the protein is about one order of magnitude lower than that for free lipids in the fluid lipid bilayer (*56*). Experiments (*49, 50, 57*) demonstrated that the degree of ordering and fluidity of the hydrocarbon chains of the bound molecules are not very different from those for the free molecules, in contrast with the initial hypotheses (*46, 47*).

Chen and Hubbell (*58*) found out experimentally that the transmembrane protein rhodopsin was dispersed in bilayers made with di-10 : 0 phosphatidylcholine, while it aggregated in di-18 : 1 *trans*-phosphatidylcholine bilayers. The configurations of the proteins in the former and latter bilayers resemble those depicted in Fig. 5(a, b), respectively. One can conclude that the perturbation of the bilayer thickness caused by the protein can lead to protein-protein attraction. Note that the width of the protein hydrophobic belt can be both smaller (Fig. 5b) and greater (Fig. 5c) than the hydrophobic thickness of the non-perturbed bilayer.

The effect of the hydrophobic region mismatch on the aggregation behaviour of proteins was studied both experimentally (*59–63*) and theoretically (*64, 65*). For instance, Lewis and Engelman (*61*) showed that bacteriorhodopsin forms aggregates in vesicles (prepared from lipids of different chain length) only when the mismatch is greater than 0.4 nm for thicker (Fig. 5b) and 1 nm for thinner (Fig. 5c)

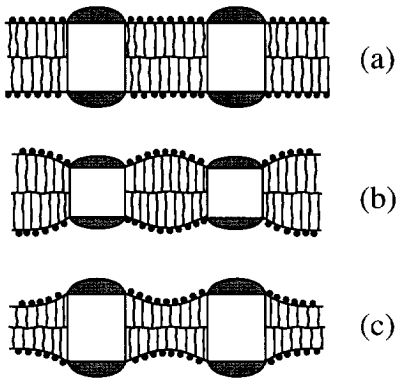

Fig. 5. Sketch of inclusions (membrane proteins) in a lipid bilayer: (a) the hydrophobic thicknesses of bilayer and inclusions coincide; (b, c) the hydrophobic thicknesses of bilayer and inclusions are different: the overlap of the deformations around the inclusions leads to a lipid mediated protein-protein interaction.

lipid bilayers. Similar protein aggregation at considerable hydrophobic mismatch was detected with other natural proteins (*59, 60, 62*) and with artificially synthesised polypeptides (*60*). It was further shown in these studies that the proteins in their own turn affect the phase transition temperature of the lipid bilayer.

In ref. *5* we propose an alternative theoretical approach to the membrane mediated interactions between inclusions, which is based on the advance in the theory of lateral capillary forces described in the previous section. We consider proteins (inclusions) of *cylindrical* shape like these depicted in Fig. 5. In this case the deformation consists of a variation of the bilayer thickness, whereas the bilayer midplane remains planar (Fig. 5b, c). Such a mode of deformation corresponds to the *squeezing mode* observed with thin liquid films (*66*).

The key for solving the aforementioned problems is the formulation of a realistic and adequate rheological model of a bilayer membrane. It is generally accepted that a lipid bilayer behaves as a 2D *fluid* at body temperature. This fact is taken into account in the 2D hydrodynamics of motion of inclusions throughout a membrane (*67*). On the other hand, the bilayer exhibits *elastic* properties in processes accompanied by extension or compression of the lipid hydrocarbon chains.

Both these effects are accounted for in the following mechanical constitutive relation for the pressure tensor τ_{ij}:

$$\tau_{ij} = -p\delta_{ij}, \quad i, j = x, y, z, \quad (i, j) \neq (z, z) \tag{5a}$$

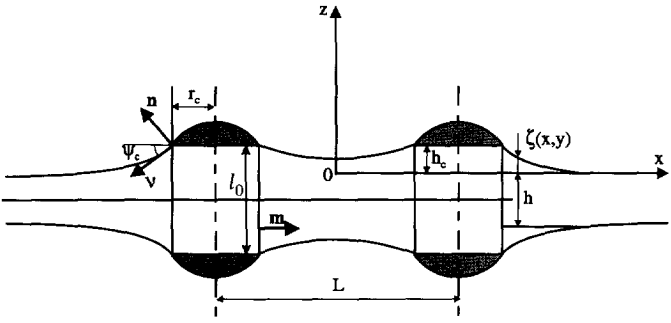

Fig. 6. Sketch of two identical cylindrical inclusions of radius r_c and hydrophobic belt width l_0 separated at an axis-to-axis distance L; h_c characterizes the "mismatch" between the width of the inclusion hydrophobic belt and the thickness of the bilayer far from the inclusion.

$$\tau_{zz} = \lambda \frac{\partial u_z}{\partial z} \tag{5b}$$

Here, δ_{ij} is the Kroneker symbol; λ is coefficient of shear elasticity, and p has the meaning of pressure characterising the bilayer as a 2D fluid: u_z is the z-component of the displacement vector $\mathbf{u}$.

The conditions for hydrostatic equilibrium and incompressibility yield (*68*)

$$\frac{\partial \tau_{ij}}{\partial x_i} = 0, \quad j = 1, 2, 3 \qquad \nabla . \mathbf{u} = 0 \tag{6}$$

($x_1 = x$, $x_2 = y$, $x_3 = z$) the coordinate system is depicted in Fig. 6. Thus, one obtains a set of 4 equations, Eqs. (6), for determining the 4 unknown functions u_x, u_y, u_z, and p.

2. Bilayer Deformation and Protein-protein Interaction

Considerations for symmetry imply that u_z must be an odd function of z which is to satisfy the boundary condition

$$u_z|_{z=\frac{h}{2}} = \zeta(x, y), \tag{7}$$

where $z = \zeta(x, y)$ describes the shape of the upper bilayer surface and h is the thickness of the non-disturbed bilayer. By imposing the boundary conditions at the bilayer surfaces one can derive (*5*) that ζ must satisfy the equation

$$\nabla_{\mathrm{II}}^2 \zeta = q^2 \zeta, \quad \nabla_{\mathrm{II}} \equiv \left(\frac{\partial}{\partial x}, \frac{\partial}{\partial y} \right) \tag{8}$$

where q is given by

$$q^2 = \frac{1}{2k_c}\left\{\tilde{\sigma}_0^2 - \left[\tilde{\sigma}_0^2 - 8k_c\frac{2\lambda}{h} - \Pi'\right]^{1/2}\right\} \approx \frac{4\lambda}{h\tilde{\sigma}_0}. \tag{9}$$

Here, $\tilde{\sigma}_0 = \sigma_0 + B_0'/h$; $B_0' = A\partial B_0/\partial A$, σ_0, B_0 and k_c are the surface tension, bending moment and the curvature elastic modulus (*69*) of the bilayer surface; A denotes area, and Π' is the derivative of disjoining pressure (see ref. *5*). The solution of Eq. (*8*) for a single cylindrical inclusion, along with the boundary condition for constant elevation at the contact line,

$$\zeta = h_c = \text{const} \quad \text{(at the contact line)} \tag{10}$$

yields

$$\zeta = \frac{h_c}{K_0(qr_c)} K_0(qr) \quad (r \geq r_c) \tag{11}$$

where r is the radial coordinate, r_c is the radius of the cylindrical inclusion and K_0 is modified Bessel function (see, *e.g.*, refs. *70, 71*).

For a couple of inclusions we find $\zeta(\mathbf{r})$ by solving numerically Eq. (*8*) in bipolar coordinates (see ref. *71*). The interaction energy between two inclusions (Fig. 6) separated at a distance L is (*5*)

$$\Delta\Omega(L) \equiv \Omega(L) - \Omega(\infty) = 4\pi(\tilde{\sigma}_0 - k_c q^2) r_c h_c [\tan\psi_c(L) - \tan\psi_c(\infty)] \tag{12}$$

where

$$\tan\psi_c(L) \equiv \frac{1}{2\pi r_c}\oint_C dl(-\mathbf{m}\cdot\nabla_{\mathrm{II}}\zeta) \tag{13}$$

represents the average meniscus slope at the contact line C. To calculate $\Delta\Omega(L)$ from Eq. (12) one must first solve numerically Eq. (8) and then substitute the calculated ζ in the right-hand side of Eq. (13). In ref. *5* we derived an asymptotic formula for $\Delta\Omega(L)$ which reads

$$\Delta\Omega(L) = 4\pi(\tilde{\sigma}_0 - q^2 k_c) q r_c h_c^2 \left[\frac{K_1(qr_c) - (1/2)qr_c K_0(qL)}{K_0(qr_c) + K_0(qL)} - \frac{K_1(qr_c)}{K_0(qr_c)}\right]. \tag{14}$$

The numerical test of Eq. (14) shows that it gives $\Delta\Omega(L)$ with good accuracy. The lateral capillary force can be obtained by differentiation:

$$F_x = -\frac{\partial \Delta\Omega}{\partial L}.$$

In our model calculations we used the parameters of the bacteriorhodopsin molecule, which has approximately cylindrical shape (see, *e.g.*, refs. *11* and *72*). The geometrical parameters of this cylindrical molecule are known from electron microscopy studies (*11*, *72*) to be $r_c = 1.5$ nm and $l_0 = 3.0$ nm (*cf.* Fig. 6). We suppose that the hydrophobic α-helix regions of the bacteriorhodopsin molecule are situated entirely inside the lipid bilayer. The respective "three-phase contact lines" are situated between the hydrophobic wall of the cylinder (formed from packed α-helix chains) and its hydrophilic parts (the bases of the cylinder). We use typical values for the bilayer parameters: $\lambda = 2 \times 10^6$ N/m^2, $\sigma_0 = 35$ mN/m and $B_0 = -3.2 \times 10^{-11}$ N (see ref. *5*).

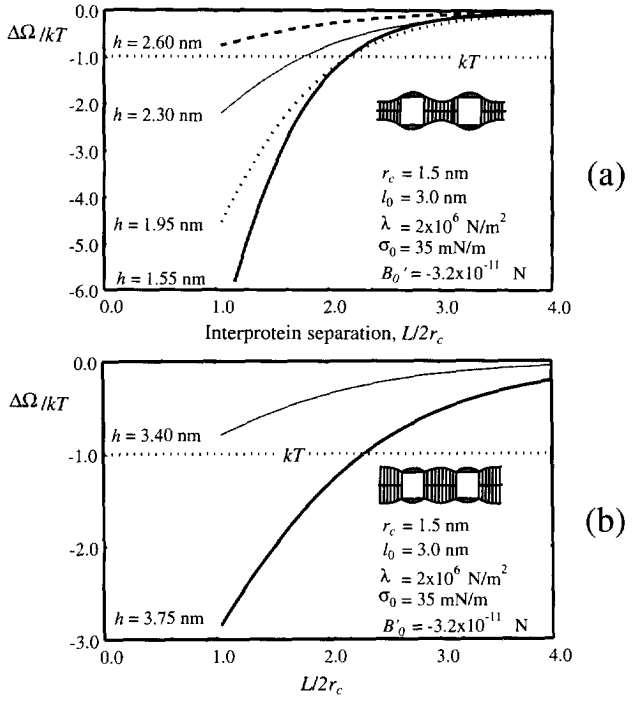

Fig. 7. Plot of the capillary interaction energy, $\Delta\Omega$, as a function of the interprotein separation, L. The different curves correspond to different values of the bilayer thickness, h. The geometrical parameters of the protein molecules are taken from ref. *27*: $r_c = 1.5$ nm and $l_0 = 3.0$ nm; besides, $\lambda = 2 \times 10^6$ N/m^2, $B_0' = -3.2 \times 10^{-11}$ N, $\sigma_0 = 35$ mN/m. The bilayer is thinner (a) or thicker (b) than the bacteriorhodopsin hydrophobic zone.

Our results on the energy of capillary interaction, Ω *vs.* $L/2r_c$ for different bilayer thickness, h, are shown in two plots: Fig. 7a for $h_c > 0$ and Fig. 7b for $h_c < 0$. The values of h (see ref. *73*) correspond to the thickness of the bilayers studied experimentally in ref. *61*. One sees that in both cases the capillary energy is negative and corresponds to attraction between the protein molecules in the bilayer. Comparing the cases when h_c has the same magnitude but the opposite signs (note that $h_c = 0.2$ nm for the curve with $h = 2.6$ nm in Fig. 7a, whereas $h_c = -0.2$ nm for the curve with $h = 3.4$ nm in Fig. 7b), one can conclude that the capillary attraction is larger in magnitude and more long-range in the case of $h_c < 0$ (thicker bilayer). This finding is consonant with the observations of Lewis and Engelman (*61*).

We compare $\Delta\Omega$ with the energy of the thermal motion, kT, for $T = 298$ K. One can see that for both $h_c > 0$ and $h_c < 0$ the interaction energy is larger than the thermal energy, kT, except for $h = 2.60$ nm and $h = 3.40$ nm corresponding to rather small values of h_c. On the contrary, for the two limiting cases, $h = 1.55$ nm and $h = 3.75$ nm the interaction energy is high enough (5–10 kT in close contact) to cause an aggregation of the membrane proteins. Only in these two limiting cases have Lewis and Engelman (*61*) observed protein aggregation.

In conclusion, we note that Fig. 7(a, b) gives an illustration of the order of magnitude and range of the protein-protein interactions, rather than a quantitative comparison between theory and experiment. The real experiment is too complicated and many parameters values are unknown. For example, the temperature (and consequently the values of σ_0, λ, *etc.*) are different in the separate experiments (*61*) with bilayers of different thickness, h.

Our model was compared with the phenomenological approach by Dan *et al.* (*74*) and relationships between the parameters of the two models were obtained (*5*).

We hope the detailed theoretical model described above will be helpful for interpretation of the processes of protein aggregation in the lipid bilayers as well as for any processes affected by the membrane stretching and bending elastic properties.

SUMMARY

To investigate the mechanism of formation of 2D arrays of protein macromolecules in liquid films we carried out model experiments with μm-sized latex particles. The direct observations revealed that the process of ordering is triggered by attractive lateral capillary forces due to

the overlap of the menisci formed around the particles. Two types of lateral capillary forces, flotation and immersion, can be distinguished, and a theory of these interactions is developed. Similar forces are operative between inclusions (proteins) incorporated in lipid membranes. We develop an appropriate model of a lipid bilayer, which is described as an elastic layer (the hydrocarbon chain region) sandwiched between two Gibbs dividing surfaces (the two headgroup regions). The range of the interaction between two cylindrical inclusions turns out to be of the order of several inclusion radii. The results, which are in qualitative agreement with the experimental observations, can be applied to the interpretation of membrane processes and mechanisms such as protein aggregation in lipid membranes.

Acknowledgments

This study was supported by the Research and Development Corporation of Japan (JRDC) under the Nagayama Protein Array Project of the program "Exploratory Research for Advanced Technology" (ERATO). The author is indebted to Profs. I.B. Ivanov and K. Nagayama for the valuable discussions and suggestions. The team members who devoted time to this study, Dr. N.D. Denkov, Dr. C.D. Dushkin, O.D. Velev, V.N. Paunov and G.S. Lazarov, are highly acknowledged.

REFERENCES

1 N.D. Denkov, O.D. Velev, P.A. Kralchevsky, I.B. Ivanov, H. Yoshimura, and K. Nagayama, *Nature*, **361**, 26 (1993); *Langmuir*, **8**, 3183 (1992).
2 P.A. Kralchevsky, V.N. Paunov, I.B. Ivanov, and K. Nagayama, *J. Colloid Interface Sci.*, **151**, 79 (1992).
3 P.A. Kralchevsky, V.N. Paunov, N.D. Denkov, I.B. Ivanov, and K. Nagayama, *J. Colloid Interface Sci.*, **155**, 420 (1993).
4 P.A. Kralchevsky and K. Nagayama, *Langmuir*, **10**, 23 (1994).
5 P.A. Kralchevsky, V.N. Paunov, N.D. Denkov, and K. Nagayama, *J. Chem. Soc. Faraday Trans.*, **91**, 3415 (1995).
6 H.W. Deckman and J.H. Dunsmuir, *Appl. Phys. Lett.*, **41**, 337 (1982).
7 H.W. Deckman, J.H. Dunsmuir, S. Garoff, J.A. McHenry, and D.G. Peiffer, *J. Vac. Sci. Technol. B*, **6**, 333 (1988).
8 S. Hayashi, Y. Kumamoto, T. Suzuki, and T. Hirai, *J. Colloid Interface Sci.*, **144**, 538 (1991).
9 C.D. Dushkin, K. Nagayama, T. Miwa, and P.A. Kralchevsky, *Langmuir*, **9**, 3695 (1993).
10 B.K. Jap, M. Zulauf, T. Scheybani *et al.*, *Ultramicroscopy*, **46**, 45 (1992).
11 R. Henderson and P.N.T. Unwin, *Nature*, **257**, 28 (1975).
12 R. Henderson, J.M. Baldwin, T.A. Ceska, F. Zemlin, E. Beckmann, and K.H. Downing, *J. Mol. Biol.*, **213**, 899 (1990).
13 P.N.T. Unwin and G. Zampighi, *Nature*, **283**, 545 (1980).
14 J.-L. Popot and J.P. Changeux, *Physiol. Rev.*, **64**, 1162 (1984).

15 C.D. Dushkin, H. Yoshimura, and K. Nagayama, *Chem. Phys. Lett.*, **204**, 455 (1993).
16 J.R. Harris, Z. Cejka, A. Wagener-Strake, W. Gebauer, and J. Markl, *Micron Microsc. Acta*, **23**, 287 (1992).
17 R. Zahn, J.R. Harris, G. Pfeifer, A. Plückthun, and W. Baumeister, *J. Mol. Biol.*, **229**, 579 (1993).
18 R.M. Glaeser, A. Zilker, M. Radermacher, H.E. Gaub, T. Hartmann, and W. Baumeister, *J. Microsc.*, **161**, 21 (1991).
19 A. Engel, *Annu. Rev. Biophys. Chem.*, **20**, 79 (1991).
20 L. Haggerty, B.A. Watson, M.A. Barteau, and A.M. Lenhoff, *J. Vac. Sci. Technol. B*, **9**, 1219 (1991).
21 R.W. Horne, *Adv. Virus Res.*, **24**, 173 (1979).
22 H. Yoshimura, S. Endo, M. Matsumoto, K. Nagayama, and Y. Kagawa, *J. Biochem.*, **106**, 958 (1989).
23 H. Yoshimura, M. Matsumoto, S. Endo, and K. Nagayama, *Ultramicroscopy*, **32**, 265 (1990).
24 T. Akiba, H. Yoshimura, and K. Namba, *Science*, **252**, 1544 (1991).
25 N. Ishii, H. Taguchi, M. Yoshida, H. Yoshimura, and K. Nagayama, *J. Biochem.*, **110**, 905 (1991).
26 K. Nagayama, *Nanobiology*, **1**, 25 (1992).
27 G.S. Lazarov, N.D. Denkov, O.D. Velev, P.A. Kralchevsky, and K. Nagayama, *J. Chem. Soc. Faraday Trans.*, **90**, 2077 (1994).
28 J.G. Riess and M. Le Blanc, *Pure Appl. Chem.*, **54**, 2383 (1982).
29 M.-J. Stébé, G. Serratrice, and J.-J. Delpuech, *J. Phys. Chem.*, **89**, 2837 (1985).
30 G. Mathis, P. Leempoel, J.-C. Ravey, C. Selve, and J.-J. Depluech, *J. Am. Chem. Soc.*, **106**, 6162 (1984).
31 M. Morita, M. Matsumoto, S. Usui *et al.*, *Colloids Surf.*, **67**, 81 (1992).
32 M.M. Nicolson, *Proc. Camb. Philos. Soc.*, **45**, 288 (1949).
33 D.Y.C. Chan, J.D. Henry, and L.R.J. White, *J. Colloid Interface Sci.*, **79**, 410 (1981).
34 W.A. Gifford and L.E. Scriven, *Chem. Eng. Sci.*, **26**, 287 (1971).
35 V.N. Paunov, P.A. Kralchevsky, N.D. Denkov, and K. Nagayama, *J. Colloid Interface Sci.*, **157**, 100 (1993).
36 V.N. Paunov, P.A. Kralchevsky, N.D. Denkov, I.B. Ivanov, and K. Nagayama, *Colloids Surf.*, **67**, 119 (1992).
37 P.A. Kralchevsky, V.N. Paunov, N.D. Denkov, and K. Nagayama, *J. Colloid Interface Sci.*, **167**, 47 (1994).
38 P.A. Kralchevsky, V.N. Paunov, and K. Nagayama, *J. Fluid Mech.*, **299**, 105 (1995).
39 C. Camoin, J.F. Roussel, R. Faure, and R. Blanc, *Europhys. Lett.*, **3**, 449 (1987).
40 O.D. Velev, N.D. Denkov, V.N. Paunov, P.A. Kralchevsky, and K. Nagayama, *Langmuir*, **9**, 3702 (1993).
41 C.D. Dushkin, P.A. Kralchevsky, H. Yoshimura, and K. Nagayama, *Phys. Rev. Lett.*, **75**, 3454 (1995).
42 C.D. Dushkin, P.A. Kralchevsky, V.N. Paunov, H. Yoshimura, and K. Nagayama, *Langmuir*, **12**, 641 (1996).
43 J.D. Robertson, *J. Cell Biol.*, **19**, 201 (1963).
44 A.K. Mitra, M.P. McCarthy, and R.M. Stroud, *J. Cell Biol.*, **109**, 755 (1989).
45 A. Baroin, A. Bienvenue, and P.F. Devaux, *Biochemistry*, **18**, 1151 (1979).
46 S. Marcelja, *Biochim. Biophys. Acta*, **455**, 1 (1976).
47 H. Schröder, *J. Chem. Phys.*, **67**, 1617 (1977).
48 J.N. Israelachvili, *Biochim. Biophys. Acta*, **469**, 221 (1977).
49 G. Benga and R.P. Holmes, *Prog. Biophys. Molec. Biol.*, **43**, 195 (1984).
50 M. Bloom, E. Evans, and O.G. Mouritsen, *Quart. Rev. Biophys.*, **24**, 293 (1991).
51 P. Jost, O.H. Grifith, R.A. Capaldi, and G. Vanderkooi, *Biochim. Biophys. Acta*, **311**, 141 (1973).
52 J.H. Davis, D.M. Clare, R.S. Hodges, and M. Bloom, *Biochemistry*, **22**, 5298 (1983).

53 M. Esmann, A. Watts, and D. Marsh, *Biochemistry*, **24**, 1386 (1985).
54 J.C. Owicki, M.W. Springgate, and H.M. McConnell, *Proc. Natl. Acad. Sci. USA*, **75**, 1616 (1978).
55 J.C. Owicki and H.M. McConnell, *Proc. Natl. Acad. Sci. USA*, **76**, 4750 (1979).
56 R.D. Pates and D. Marsh, *Biochemistry*, **26**, 29 (1987).
57 E. Favre, A. Baroin, A. Bienvenue, and P.F. Devaux, *Biochemistry*, **18**, 1156 (1979).
58 Y.S. Chen and W.L. Hubbel, *Exp. Eye Res.*, **17**, 517 (1973).
59 J. Davoust, A. Bienvenue, P. Fellmann, and P.F. Devaux, *Biochim. Biophys. Acta*, **596**, 28 (1980).
60 J.C. Huschilt, R.S. Hodges, and J.H. Davis, *Biochemistry*, **24**, 1377 (1985).
61 B.A. Lewis and D.M. Engelman, *J. Mol. Biol.*, **166**, 203 (1983).
62 J. Riegler and H. Möhwald, *Biophys. J.*, **49**, 1111 (1986).
63 J. Peschke, J. Riegler, and H. Möhwald, *Eur. Biophys. J.*, **14**, 385 (1987).
64 O.G. Mouritsen and M. Bloom, *Biophys. J.*, **46**, 141 (1984).
65 M.M. Sperotto and O.G. Mouritsen, *Eur. Biophys. J.*, **19**, 157 (1991).
66 J.G.H. Joosten, "Thin Liquid Films," ed. by I.B. Ivanov, M. Dekker, New York, p. 569 (1988).
67 S.J. Bussell, D.L. Koch, and D.A. Hammer, *J. Fluid Mech.*, **243**, 679 (1992).
68 L.D. Landau and E.M. Lifshitz, "Theory of Elasticity," Pergamon Press, Oxford (1970).
69 P.A. Kralchevsky, J.C. Eriksson, and S. Ljunggren, *Adv. Colloid Interface Sci.*, **48**, 19 (1994).
70 M. Abramowitz and I.A. Stegun, "Handbook of Mathematical Functions," Dover, New York (1965).
71 G.A. Korn and T.M. Korn, "Mathematical Handbook," McGraw-Hill, New York (1968).
72 P.N.T. Unwin and R. Henderson, *J. Mol. Biol.*, **94**, 425 (1975).
73 E. Sackmann, R. Kotulla, and F.J. Heiszler, *Can. J. Biochem. Cell Biol.*, **62**, 778 (1984).
74 N. Dan, P. Pincus, and A. Safran, *Langmuir*, **9**, 2768 (1993).